Heliyon 10 (2024) e39493

Contents lists available at ScienceDirect

Heliyon

journal homepage: www.cell.com/heliyon

Research article

Bioactivity of biogenic silver/silver chloride nanoparticles from *Maranta arundinacea* rhizome extract: Antibacterial and antioxidant properties with anticancer potential against Ehrlich ascites carcinoma and human breast cancer cell lines

Md. Ruhul-Amin [a,b], Md. Abdur Rahman [a], Nisa Khatun [a], Imtiaj Hasan [a], Syed Rashel Kabir [a], A.K.M. Asaduzzaman [a,*]

[a] *Department of Biochemistry & Molecular Biology, Faculty of Science, University of Rajshahi, Rajshahi, 6205, Bangladesh*
[b] *Department of Biochemistry and Molecular Biology, Trust University, Barisal, 8200, Bangladesh*

ARTICLE INFO

Keywords:
Anticancer potential
Maranta arundinacea rhizome
Silver/silver chloride nanoparticles

ABSTRACT

Introduction: This study explores the synthesis and characterization of silver/silver chloride nanoparticles (Ag/AgCl-NPs) using *Maranta arundinacea* rhizome extract and evaluates their bioactivities, including antibacterial, antioxidant, and anticancer potentials.

Methods: The synthesis of Ag/AgCl-NPs was initially confirmed by a color change and a sharp peak at 463 nm in UV–visible spectroscopy. Further characterization was conducted using scanning electron microscopy (SEM), X-ray powder diffraction (XRD), and fourier transform infrared spectroscopy (FTIR). Antibacterial properties were checked against four pathogenic bacteria (*Shigella boydii, Escherichia coli, Shigella dysenteriae,* and *Staphylococcus aureus*), and antioxidant activities were assessed using DPPH (2,2-diphenyl-1-picrylhydrazyl) and ABTS (2,2-azino-bis-3-ethylbenzothiazoline-6-sulphonic acid) assay. In addition, the anticancer potential was evaluated *in vitro* using MTT (3-(4, 5-dimethylthiazolyl-2)-2, 5-diphenyltetrazolium bromide) colorimetric assay and *in vivo* using the mouse models. Finally, toxicity was determined by employing the brine shrimp nauplii lethality assay.

Results: Ag/AgCl-NPs most effectively inhibited the growth of *Staphylococcus aureus*, showing maximum zone of inhibition and 7 μg/mL of minimum inhibitory concentration (MIC), and prevented the biofilm formation by *Escherichia coli* at 40 μg/mL. They displayed antioxidant activities against DPPH and ABTS with IC_{50} values of 90.65 and 24.34 μg/mL, respectively. *In vitro*, they inhibited 61.96 % EAC and 49.63 % MCF-7 cells growth at 32 and 128 μg/mL, respectively. Subsequently, inhibition rates of EAC cells growth in mice were measured as 38.30 %, 57.38 %, and 31.81 % after employing 2.5, 5, and 10 mg/kg/day of Ag/AgCl-NPs, respectively. Moreover, Ag/AgCl-NPs treated mice were found to carry more apoptotic EAC cells with distorted morphology. Treated mice showed decreased tumor weight, increased mean survival time, and a lifespan increase of up to 30 %, with improved hematological parameters. Later, Ag/AgCl-NPs exhibited moderate toxicity with an LC_{50} value of 208.41 μg/mL in brine shrimp nauplii lethality assay.

Conclusion: The promising antibacterial, antioxidant, and anticancer activities along with mild toxicity suggest the potential biomedical uses of *Maranta arundinacea* rhizome extract-mediated Ag/AgCl-NPs.

* Corresponding author: jonyasad2005@ru.ac.bd

https://doi.org/10.1016/j.heliyon.2024.e39493
Received 3 May 2024; Received in revised form 20 September 2024; Accepted 15 October 2024
Available online 16 October 2024

1. Introduction

Nanotechnology is an outstanding field of current research that deals with the synthesis, characterization, and application of nanoparticles, which are tiny substances ranging from 1 to 100 nm in size [1]. Apart from small size, the nanoparticles also have numerous characteristics like comparatively larger surface area to volume ratio, intense reactivity or stability in any chemical process, and prolonged mechanical potency. Because of these exceptional features, nanoparticles exhibit some unparalleled physical, chemical, and biological properties at the nanoscale range compared to other bigger particles. These properties have made nanoparticles exclusive and enabled their uses in a variety of fields [2]. Some of the major promising applied fields of nanoparticles are drugs and medications, manufacturing and materials, environment, electronics, energy harvesting, and mechanical industries [3].

Nanoparticles can be synthesized chemically, physically, or biologically. While chemical and physical methods can produce pure and well-defined nanoparticles, they are costly, energy swallowing, and environmentally hazardous. Biological methods using microorganisms, enzymes, fungi, and plants are the alternatives to chemical and physical methods. Particularly, plant extracts facilitate the formation of stable metal nanoparticles by faster reduction of metal ions. Nowadays, different metallic nanomaterials are being produced employing metals such as copper, zinc, titanium, magnesium, gold, alginate, and silver [4–6]. However, the applications of silver nanoparticles (AgNPs) have recently drawn special attention because of their unique and attractive physical, chemical, and biological features such as chemical stability, catalytic activity, numerous medicinal effects, protective activity against infective microorganisms, highest electrical and thermal conductivity, and low sensitizing temperature. AgNPs also show certain functions regarding toxicity, surface plasmon resonance (SPR), and electrical resistance [1,7]. They have various applications including the medical, food industries, households, consumer products, industrial purposes, pharmaceutical industries, healthcare-related products, cosmetics, medical devices coatings, textiles, and keyboards. Nanoparticles, especially AgNPs are one of the well-known candidates of nanomedicine which is now the major emerging field of nanotechnology. As candidates for nanomedicine, AgNPs serve as antimicrobial agents, antibiotics, anti-inflammatory agents, biosensors, and optical sensors, and are used in drug delivery, biomedical devices, wound dressings, orthopedics, and diagnostics. Notably, they enhance the tumor-killing effects of various anticancer drugs [8–10].

Multidrug resistance in many pathogenic bacteria causes numerous deaths globally every year and is becoming an increasingly urgent health issue day by day. AgNPs emerge as a worthy solution to this issue, as they have been reported to prevent infections caused by these drug-resistant bacteria [11]. Several studies informed about the antibacterial activity of plant-mediated Ag/AgCl-NPs [12,13]. Biogenic Ag/AgCl-NPs as antioxidants have also been reported to play a significant role in the scavenging of life-threatening free radicals [14,15].

Cancer is a widespread group of diseases that causes numerous metabolic alterations and signaling mechanisms within cells, for instance, abnormal cellular growth, breakdown of genetic materials, angiogenesis, and metastasis. The most formidable nature of cancer is metastasis which has made it a prime cause of death globally [7,16,17]. As the world population is growing and lifestyle change contributes to increased cancer risk, it is expected that the chances of getting cancer, the number of new cases, and the mortality rate of cancer will grow rapidly [18]. Some conventional therapeutic strategies for cancer treatment are chemotherapy, surgery, and radiation therapy [19]. Chemotherapy is standard for various types of cancers, though the majority of chemotherapeutic drugs showed limited impact and adverse effects including drug resistance, trouble in dosage fixation, less specificity, and quick drug metabolism [20,21]. Thus, identifying novel anticancer drugs with minimal or no side effects has become an obligate goal of many researchers [22]. Aiming for this, many researchers are exploring the use of Ag/AgCl-NPs produced through cost-effective, rapid, and nontoxic green biosynthesis methods using plant extracts as a potential anticancer agent alternative to traditional anticancer agents [12,23,24]. Several articles have reported the potential of plant leaf, root, bark, or fruit extract-mediated Ag/AgCl-NPs against different cancers [12,24–27].

In this study, we synthesized Ag/AgCl-NPs using the rhizome extract of *Maranta arundinacea*, an important starchy medicinal plant belonging to the Marantaceae family and known as arrowroot used in traditional foods and medicine. Taxonomically, it falls under the order Zingiberales and class Monocots. This tropical species is native to the Caribbean and South America, but it has been distributed throughout other tropical regions, like Southeast Asia, Australia, etc. Morphologically, this is a perennial herbaceous plant, growing to a height of 0.5–1 m. Its starchy, fleshy rhizome measures about 2.5–5 cm in thickness and 20–45 cm in length, with a curved, arrow-like shape, covered by overlapping scales. Additionally, this plant has long ovate leaves and produces small cream to white compound flowers [28]. It has numerous biological activities, for instance, immune-stimulatory, anti-ulcerogenic, vibriocidal, and anti-inflammatory effects. Moreover, it has been traditionally used to control diseases, like diabetes, high blood pressure, cardiovascular disease, diarrhea, etc. [28,29]. It contains many phytochemicals such as carbohydrates, proteins, and polyphenolic compounds [29,30]. Polyphenolic compounds like flavonoids and tannins present in this plant could be responsible for its several biological properties, for instance antibacterial, antioxidant, and anticancer effects. These phytochemicals could also be worked as capping agents during Ag/AgCl-NPs synthesis [31,32]. The methanolic extracts from *Maranta arundinacea* were previously reported to show antibacterial activity against *Staphylococcus aureus* [33]. However, the antioxidant, antibacterial, and anticancer activities of *Maranta arundinacea* rhizome extract-mediated Ag/AgCl-NPs have not been reported yet. That's why our study is the first to select *Maranta arundinacea* rhizome for this purpose.

2. Materials and methods

2.1. Chemicals and Reagents

Silver nitrate ($AgNO_3$), Hoechst-33342, Propidium Iodide, Bovine serum albumin, RPMI-1640 (Roswell Park Memorial Institute-1640), and MTT were purchased from Sigma-Aldrich (USA). Iso-propanol was purchased from Roth (Germany). Potassium bromide (KBr), Bacto yeast extract, Bacto peptone, Sodium chloride (NaCl), Sodium tetra-borate, and Chloroform were procured from Merck (Germany). Nutrient agar and Standard antibiotic (Erythromycin) were purchased from Himedia (India). All other chemicals used throughout the experiments were of the highest analytical grade.

2.2. Sample collection and preparation

Fresh *Maranta arundinacea* rhizome was bought from the local market of Natore, Rajshahi, Bangladesh. Then it was properly washed under tap water to remove debris and other unnecessary particles. After that, the sample was again washed and rinsed with deionized water for several times. Further, the sample was cut into small pieces and dried under sunlight for about 15 days to remove the water content and finally, the dried sample was blended to produce powder.

2.3. Preparation of extract

The powder (2 %) was mixed with deionized water and heated with continuous stirring at 85 °C for 15 min. Next, the homogenate was clarified using a clean muslin cloth and centrifuged at 7000 rpm at 4 °C for 15 min to prepare clear *M. arundinacea* rhizome extract. Further, the extract was stored at 4 °C for subsequent steps of Ag/AgCl-NPs synthesis [34].

2.4. Ag/AgCl-NPs synthesis

For the synthesis of Ag/AgCl-NPs, clear *M. arundinacea* rhizome extract was taken in 6 test tubes (2 mL/tube), and different volumes of 1 M $AgNO_3$ stock solution were poured into the test tubes to gain the final concentrations of $AgNO_3$ at 1, 2, 3, 4, 5, and 6 mM in each respective test tubes. Subsequently, the test tubes were gently shaken before being kept in the sunlight for different periods such as 5, 10, 20, 40, 80, 160, and 320 min [35]. The change of the light reddish color of the extract into the dark brown color primarily indicated the formation of Ag/AgCl-NPs.

2.5. UV–visible spectra analysis

From each test tube, 0.2 mL of Ag/AgCl-NPs in 2 mL deionized water was subjected to UV–visible spectroscopic analysis (UV-1650 PC, Shimadzu, Japan) at the wavelength ranging from 250 to 750 nm [34].

2.6. Processing of Ag/AgCl-NPs

The reaction mixture that provided the sharpest peak at UV–visible spectra analysis was centrifuged at 12,000 rpm for 15 min at 4 °C. Afterward, the obtained pellet was again dispersed in deionized water. Subsequently, this mixture was centrifuged for five times to remove excess silver ions. A part of the colloidal Ag/AgCl-NPs was lyophilized to measure the concentration and the rest of the colloidal nanoparticles were stored at 4 °C for further characterization [34].

2.7. SEM analysis

SEM (ZEISS, EVO 18SEM, Germany) was used for the determination of the shape and size of the synthesized Ag/AgCl-NPs. By the process of sputtering, the powder form of Ag/AgCl-NPs was coated with gold-palladium and placed onto the sample holder. After air drying, the SEM observation was performed [36]. By using the image ''J'' software program the average size of Ag/AgCl-NPs was determined.

2.8. XRD analysis

An X-ray diffractometer was used to characterize the powdered form of synthesized Ag/AgCl-NPs. Using CuKα radiation (λ = 1.54060 Å) the diffraction pattern was obtained with a nickel monochromator from 20° to 80° [37].

2.9. FTIR analysis

FTIR was used for the identification of functional groups in *M. arundinacea* rhizome extract as well as synthesized Ag/AgCl-NPs. It was done at a resolution of 4 cm^{-1} after mixing the Ag/AgCl-NPs with KBr. The spectra were recorded in the wavelength range from 4000 to 225 cm^{-1} [12]. This experiment was performed at the central science laboratory, University of Rajshahi, Bangladesh.

2.10. Antibacterial assay

2.10.1. Antibacterial assay by disc diffusion method

The antibacterial activity of synthesized Ag/AgCl-NPs was investigated by the paper disc diffusion method [38]. *Shigella boydii, Escherichia coli, Shigella dysenteriae,* and *Staphylococcus aureus* were used as test microorganisms in this assay. Paper discs 5 mm in diameter containing three different Ag/AgCl-NPs and $AgNO_3$ concentrations (10, 20, and 40 μg/disc) and erythromycin (15 units/disc) as a standard antibiotic were positioned on sterilized agar plates. The bacterial suspension was spread out on a plate before putting paper discs. The diameter of each inhibitory zone (mm) was determined after incubation at 37 °C for 24 h.

2.10.2. Determination of minimum inhibitory concentration (MIC)

The MIC of synthesized Ag/AgCl-NPs against different bacteria was determined as per the method of Arfin et al. [39] with a slight change. For this study, *Shigella boydii, Escherichia coli, Shigella dysenteriae,* and *Staphylococcus aureus* were taken in different test tubes and kept overnight for growth. Then different concentrations of Ag/AgCl-NPs (30-1 μg/mL) were added with 2 mL bacterial suspension where the control group didn't contain Ag/AgCl-NPs. The test tubes were then permitted to be kept overnight at 37 °C in a bacteriological incubator. The existence of metabolically active bacterial cells was confirmed by comparing the absorbance of each test tube at 640 nm where the fresh media containing no bacteria was used as blank. The minimum concentration of Ag/AgCl-NPs at which we observed no bacterial growth was noted as the MIC. The bacterial cells growth inhibition (%) was calculated by using the following formula:

$$\text{Bacterial cells growth inhibition (\%)} = \{(Ac - As)/Ac\} \times 100$$

Where, Ac = Absorbance of control (without Ag/AgCl-NPs) and As = Absorbance of sample.

2.10.3. Antibiofilm assay

Antibiofilm assay was performed by observing biofilm formed by *E. coli* bacteria in test tubes with and without synthesized Ag/AgCl-NPs according to a published method [38] with a slight modification. 40 μL of bacterial suspension was mixed with different concentrations (10, 20, 40, and 80 μg/mL) of Ag/AgCl-NPs in small glass test tubes containing 2 mL of sterile nutrient broth media. A test tube without Ag/AgCl-NPs was used as a control. The tubes were incubated at 37 °C and the film formation was checked after 24 h and extended up to 96 h at different time intervals.

2.11. Antioxidant study

2.11.1. DPPH free radical scavenging activity assay

The DPPH scavenging activity of synthesized Ag/AgCl-NPs and ascorbic acid as standard was determined as per the protocol [40] with slight modification. At first, 1.0 mL aliquot of sample and standard solution at various concentrations (6.25, 12.50, 25, 50, 75, and 100 μg/mL) was added to the test tubes and then mixed 2.0 mL of 0.1 mM DPPH solution in each test tube. The mixture was kept at room temperature in the dark for 30 min after vortexing. After that, absorbance was measured by UV–vis spectrophotometer at 517 nm. A control solution was prepared with 2 mL of methanol and Ag/AgCl-NPs. Ascorbic acid was used as the standard to determine the antioxidant activity of Ag/AgCl-NPs by using the following equation.

$$\text{\% of DPPH scavenging assay} = \{(Ac - As)/Ac\} \times 100$$

Where Ac = Absorbance of control/blank, and As = Absorbance of the samples/standard.

2.11.2. ABTS free radical scavenging activity assay

According to the procedure described in a previous article [41], ABTS assay was performed. The multiple concentrations (6.25, 12.5, 25, 50, 75, and 100 μg/mL) of Ag/AgCl-NPs and ascorbic acid as standard were used for this study. The following equation was used to calculate ABTS scavenging activity.

$$\text{\% of ABTS scavenging assay} = \{(Ac - As)/Ac\} \times 100$$

Where Ac = Absorbance of control/blank, and As = Absorbance of the samples/standard.

2.12. In vitro anticancer activity against EAC and MCF-7 cells

EAC and MCF-7 cells growth inhibitions by 4–128 μg/mL of synthesized Ag/AgCl-NPs were performed *in vitro* by MTT colorimetric assay [42].

2.13. Experimental animals and ethical clearance

We collected male, 8–9 weeks old, 25–30 gm weight Swiss albino mice from the Department of Pharmacy, Jahangirnagar University, Dhaka, Bangladesh and it was sheltered in cages (6 mice/cage) under an equal light/dark cycle with a continuous supply of food and water. *In vivo* experimental protocols were granted by the Institutional Animal, Medical Ethics, Bio-safety and Bio-security

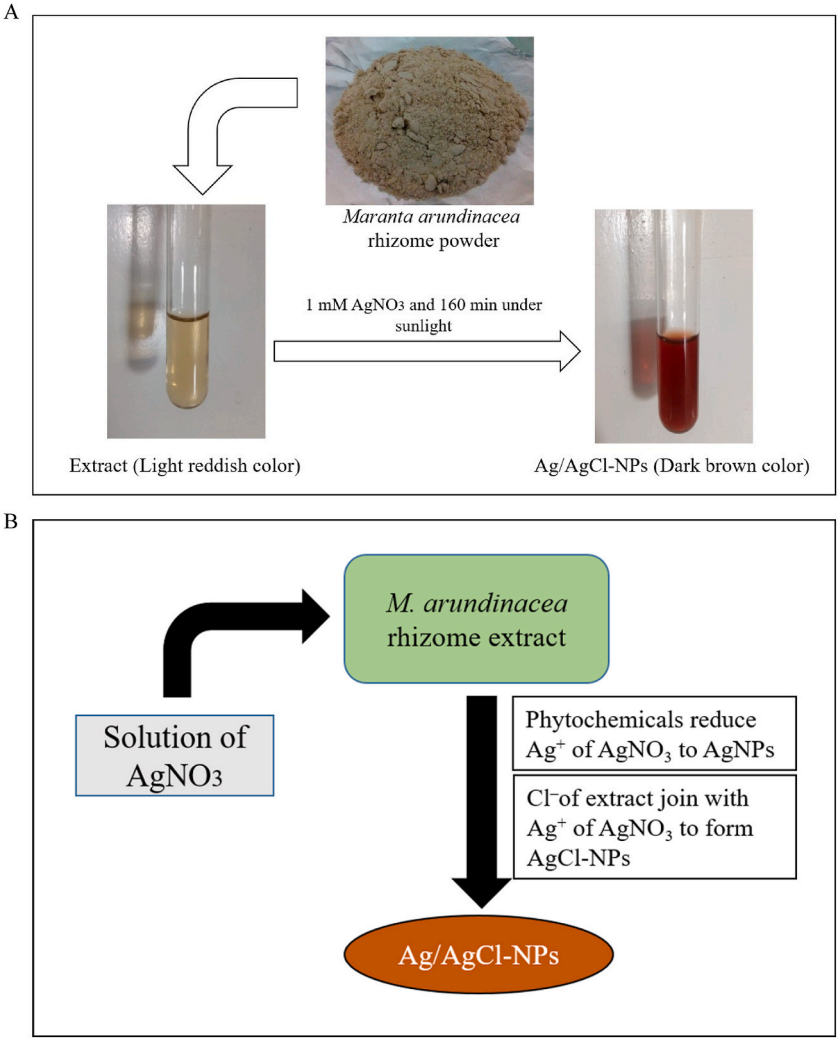

Fig. 1. (A) Synthesis of *Maranta arundinacea* rhizome extract-mediated Ag/AgCl-NPs by changes of color after the reaction at suitable conditions, and (B) Possible mode of Ag/AgCl-NPs formation.

Committee (IAMEBBC) for Experimentations on Animals, Human, Microbes and Living Natural Sources, Memo No: 249(35)/320/IAMEBBC/IBSc, Institute of Biological Sciences (IBSc), University of Rajshahi, Bangladesh as well as confirmed to ARRIVE guideline.

2.14. In vivo anticancer potential assay

2.14.1. In vivo EAC cells growth inhibition assay

We used EAC cells to propagate in Swiss albino mice intraperitoneally in the animal house of our department biweekly. Next, EAC cells were collected in saline from 7-day-old tumor-bearing mice. In exact, 1×10^6 EAC cells in 0.1 mL of saline were injected intraperitoneally in mice and kept at room temperature for tumor inoculation. After 24 h of EAC cells inoculation, total mice were subdivided into four groups where six mice were in each group and three of these groups were injected intraperitoneally with synthesized Ag/AgCl-NPs at the doses of 2.5, 5, and 10 mg/kg/day and another group was used as control. The subsequent steps were conducted according to the method described in two recently published articles [26,43].

2.14.2. Determination of average tumor weight and mean survival time

Twenty-four Swiss albino mice were injected intraperitoneally with EAC cells in the same way described above and randomly separated into four groups (six mice per group). After 24 h, Ag/AgCl-NPs were injected intraperitoneally into three groups at the doses of 2.5, 5, and 10 mg/kg/day for ten successive days and the fourth group was considered as control. The weight of each mouse was taken up to 20 days of EAC cells inoculation and survival time (days) was noted for each mouse. Subsequent steps were done as per the method [43].

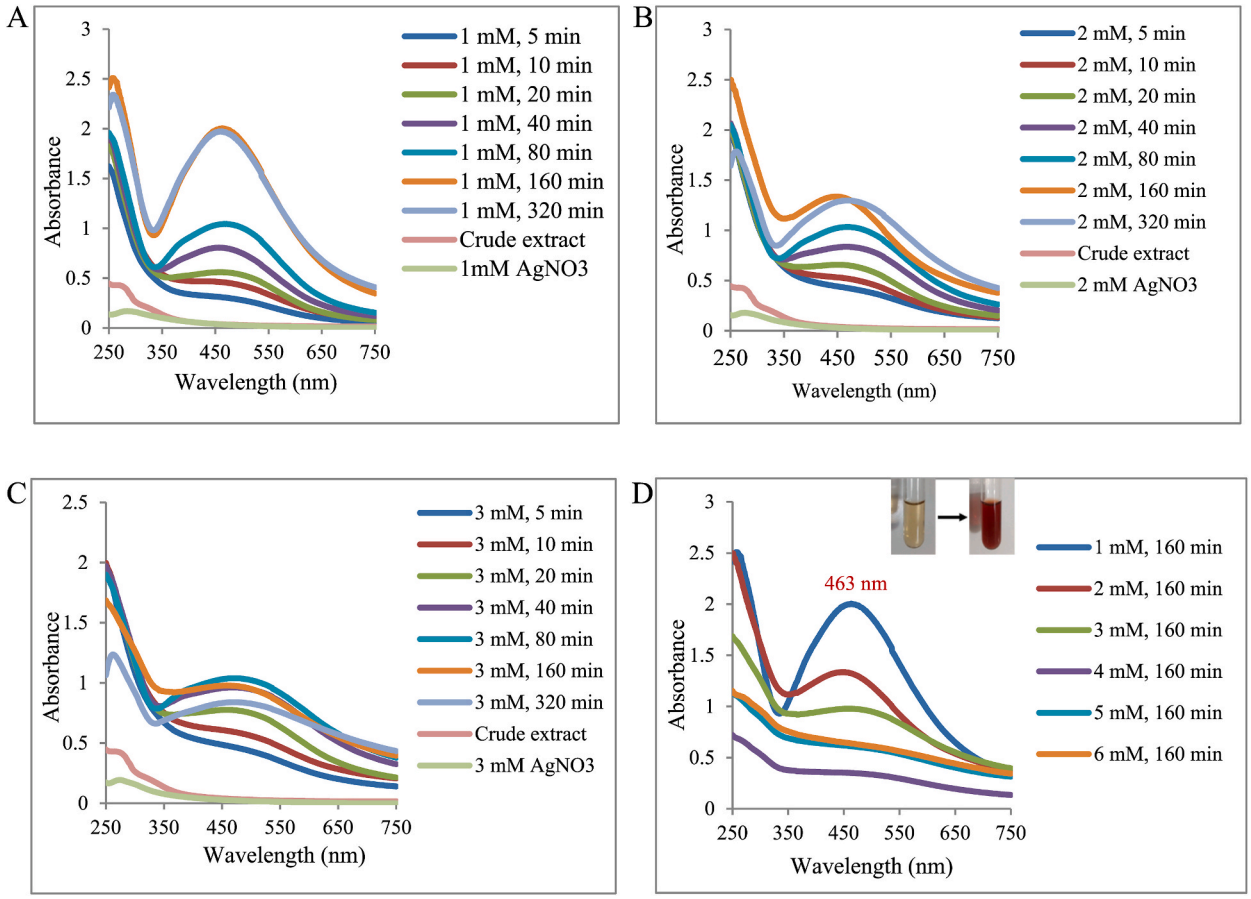

Fig. 2. UV–visible spectra of synthesized Ag/AgCl-NPs at (A) 1 mM $AgNO_3$ for different reaction times, (B) 2 mM $AgNO_3$ for different reaction times, (C) 3 mM $AgNO_3$ for different reaction times, and (D) Different concentrations of $AgNO_3$ for 160 min (The color change and the highest and sharpest absorbance peak at 463 nm indicate the completion of Ag/AgCl-NPs synthesis).

2.14.3. Morphological study of EAC cells using Hoechst-33342 and propidium iodide

Cells morphology was studied following the procedure of Arfin et al. [39]. EAC cells were collected from the mice after five consecutive days of treatment both with and without synthesized Ag/AgCl-NPs and washed thrice with PBS through centrifugation at 4 °C and 1200 rpm for 3 min. Next, 0.1 mg/mL of 5 μL of Hoechst-33342 was used to stain the cells and kept in the dark for 20 min at 37 °C temperature. Subsequently, 3 μL of propidium iodide was added 5 min before the observation of morphological alterations of EAC cells under a fluorescent microscope.

2.14.4. Determination of hematological parameters

Another six mice grown in the same conditions were taken here as a normal mice group along with the previous three treated groups and a control group used for determination of average tumor weight and mean survival time. To check the hematological parameters, the total RBC and WBC were counted under a light microscope as well as percentage of hemoglobin was measured by a Sahil hemometer on the 12th day of EAC cells inoculation using freely flowing tail vein blood of each group of mice.

2.15. Cytotoxicity assay

The brine shrimp nauplii cytotoxicity test was carried out as per the protocol [23]. Exact, 10, 20, 40, 80, 160, and 320 μg of synthesized Ag/AgCl-NPs containing 1 mL of artificial seawater were placed in each test tube, and then added 10 brine shrimp nauplii. After that, it was kept under a continuous light regime at 30 °C for 24 h. Finally, the numbers of dead and alive nauplii were counted in each test tube to calculate the mortality rate by a method [44].

2.16. Statistical analysis

The experimental results were expressed as the mean ± SD (Standard deviation). Data were analyzed using one-way ANOVA followed by Dunnett's *t*-test in GraphPad Prism Version 8.0.2 (263), and significant differences among groups were determined using

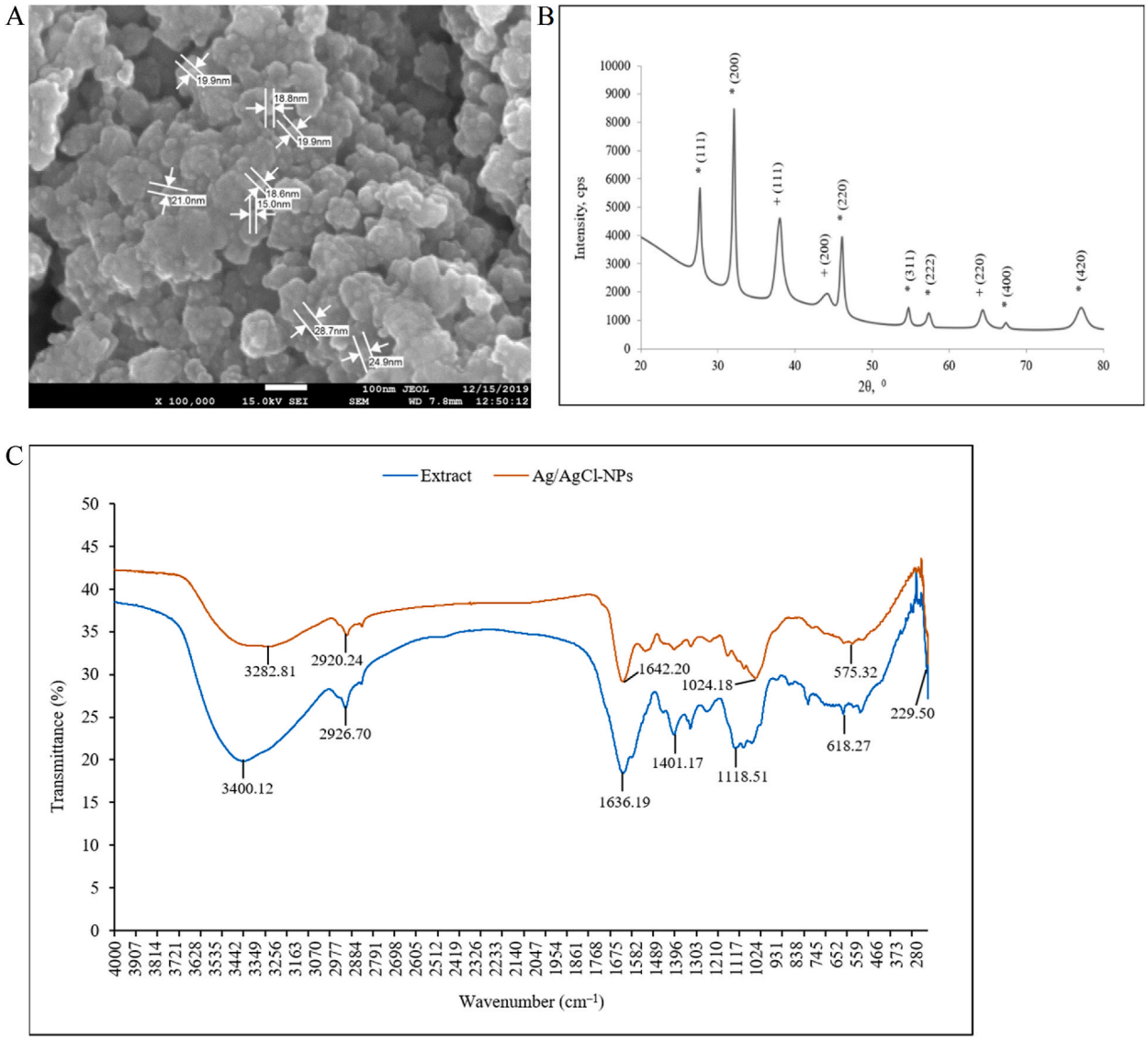

Fig. 3. (A) SEM image of synthesized Ag/AgCl-NPs, (B) XRD pattern of synthesized Ag/AgCl-NPs. (+) and (*) indicate AgNPs and AgCl-NPs, respectively, (C) FTIR spectrum of *Maranta arundinacea* rhizome extract, and synthesized Ag/AgCl-NPs.

the Tukey post hoc test in IBM SPSS Statistics Version 29.0.2.0 (20). Data were significant when $P < 0.05$.

3. Results and discussion

3.1. Synthesis of Ag/AgCl-NPs

The generation of a dark-brown colored opaque solution after the incubation of light reddish-colored transparent *M. arundinacea* rhizome extract and 1 mM of $AgNO_3$ for 160 min under sunlight primarily confirmed the formation of Ag/AgCl-NPs (Fig. 1A). This color change was occurred due to the surface plasmon resonance excitation of Ag/AgCl-NPs. The bioactive phytochemical compounds existing in the aqueous solution of *M. arundinacea* rhizome extract reduced the Ag^+ of $AgNO_3$ to Ag^0 during the formation of AgNPs, and Cl^- present in extract joined with Ag^+ to from AgCl-NPs (Fig. 1B) [20,32].

3.2. Characterization of synthesized Ag/AgCl-NPs

3.2.1. UV–visible spectra analysis

After analyzing the UV visible spectra of synthesized Ag/AgCl-NPs at 1 mM $AgNO_3$ and different reaction times (Fig. 2A), we

observed the highest peak for the reaction mixture containing 1 mM $AgNO_3$, which was exposed to proper sunlight for 160 min. Subsequently, we examined the UV–visible spectra at 2 mM (Fig. 2B) and 3 mM (Fig. 2C) $AgNO_3$ and different reaction times. However, we didn't observe any peak as high and sharp as the one obtained under the condition of 1 mM $AgNO_3$ and 160 min reaction time. As a consequence, we considered the optimal reaction time to be 160 min. Furthermore, we checked the UV–visible spectra at different $AgNO_3$ concentrations using the optimized reaction time of 160 min (Fig. 2D). Nonetheless, the highest and sharpest absorbance peak at 463 nm was consistently found with 1 mM $AgNO_3$ and 160 min reaction time. This sharp absorbance peak is a characteristic of the surface plasmon resonance effect of Ag/AgCl-NPs. Plasmon resonance for Ag/AgCl-NPs typically occurs in the visible region, with between 400 and 500 nm depending on particle shape and size [45]. Peak at 463 nm also indicates the formation of spherical and homogenously distributed Ag/AgCl-NPs [5]. Srinivas et al. [46] found the highest absorbance peak at 469 nm for *Clitoria ternatea* flower-mediated Ag/AgCl-NPs.

3.2.2. SEM analysis

The shape of synthesized Ag/AgCl-NPs was almost spherical with approximately 20.85 nm of average size as determined by SEM (Fig. 3A). Majority of the plant-mediated Ag/AgCl-NPs are spherical [1]. Few plant-mediated Ag/AgCl-NPs were reported to be around 21 nm in average size [47,48].

3.2.3. XRD analysis

The crystalline nature of the dry powder form of the synthesized Ag/AgCl-NPs was analyzed by XRD. XRD pattern displayed three distinct peaks at 38°, 44.17° and 64.27° resembling the crystallographic planes (111), (200), and (220), respectively, indicating the formation of face-centered cubic (FCC) structure of AgNPs (JCPDS, file: 03-065-2871). Likewise, the Bragg reflections at 27.62°, 32.046°, 46.058°, 54.69°, 57.25°, 67.25°, and 77.03° corresponding to the crystallographic planes (111), (200), (220), (311), (222), (400), and (420), respectively (JCPDS file: 00-031-1238), which also indicated the formation of face-centered cubic structured AgCl-NPs (Fig. 3B). Ag^+ was found to be presented in the form of silver chloride. Peaks of silver chloride (AgCl) indicated the formation of AgCl-NPs [35]. At the very beginning, AgCl-NPs could be formed because of the reaction between Ag^+ and Cl^- in the reaction mixture coming from $AgNO_3$ and phytochemicals of the aqueous rhizome extract of *M. arundinacea*, respectively. Throughout the formation of Ag/AgCl-NPs, these phytochemical compounds performed as reducing agents to reduce Ag^+ to metallic Ag as well. At first, Ag^+ formed a transitional complex with -OH groups of phenolic and flavonoid compounds originating from the *M. arundinacea* rhizome extract. This transitional complex participated in an oxidation reaction to reduce Ag^+ to AgNPs [49].

3.2.4. FTIR analysis

FTIR was used to determine possible functional groups in *M. arundinacea* rhizome extract and synthesized Ag/AgCl-NPs, which are responsible for the bio-reduction of Ag^+ into Ag/AgCl-NPs. FTIR spectrum of *M. arundinacea* rhizome extract showed seven major peaks at 3400.12, 2926.70, 1636.19, 1401.17, 1118.51, 618.27, and 229.50 cm^{-1} (Fig. 3C). At the same time, five major peaks were found at 3282.81, 2920.24, 1642.20, 1024.18, and 575.32 cm^{-1} for the synthesized Ag/AgCl-NPs (Fig. 3C). The existence of large peaks at 3400.12 and 3282.81 cm^{-1} for *M. arundinacea* rhizome extract and Ag/AgCl-NPs, respectively might be due to the -OH stretching of alcohols and phenols or bending stretching of hydrogen-bonded alcohols and phenols. These bonds could also be formed due to the stretching of -OH in proteins, enzymes or polysaccharides presented both in the extract and Ag/AgCl-NPs [50]. Because of −CH stretching of alkanes or carbonyl groups and secondary amines, weak peaks appeared at 2926.70 and 2920.24 cm^{-1} for *M. arundinacea* rhizome extract and Ag/AgCl-NPs, respectively [23,50]. At the same time, another strong peaks at 1636.19 and 1642.20 cm^{-1} for extract and Ag/AgCl-NPs, correspondingly due to the bending vibrations of the amide I group and informed the possible binding of SNPs with the proteins present in the extract and Ag/AgCl-NPs [50,51]. Medium peaks at 1118.51 and 1024.18 cm^{-1} were due to the C-O stretching of esters or C-N stretching vibrations of amines [50]. Weak peaks at 618.27 and 575.32 cm^{-1} possibly indicated the α-glucopyranose rings deformation of carbohydrates or C-Cl stretching modes of alkyl halides in extract and Ag/AgCl-NPs [51,52]. The peaks at 1401.17 cm^{-1} and 229.50 cm^{-1} were in the extract but disappeared in the Ag/AgCl-NPs which might have happened due to the reaction. The relative FTIR analysis of *M. arundinacea* rhizome extract and synthesized Ag/AgCl-NPs suggested that both of them shared some particular common functional groups, and probably −OH groups were responsible for the reduction of Ag^+ to Ag^0 [53].

3.3. Antibacterial studies of synthesized Ag/AgCl-NPs

3.3.1. Antibacterial activity of synthesized Ag/AgCl-NPs by disc diffusion method

Among four tasted pathogenic bacteria, *Staphylococcus aureus* (gram-positive) was the most sensitive to Ag/AgCl-NPs, as evidenced by the largest zones of growth inhibition, measuring 14.25 ± 0.95, 15.75 ± 0.50, and 18.00 ± 1.41 mm at the doses of 10, 20, and 40 μg/disc, respectively. Conversely, the standard antibiotic (15 units of erythromycin) was the least effective against *Staphylococcus aureus* compared to other bacteria, showing the smallest zone of growth inhibition of 18.25 ± 0.95 mm. However, standard antibiotics exhibited more efficacy against gram-negative bacteria, as supported by the zones of growth inhibition of 20.25 ± 0.50, 19.75 ± 0.57, and 18.75 ± 0.50 mm against *Shigella boydii*, *Escherichia coli*, and *Shigella dysenteriae*, respectively. Overall, according to the entire set of results, synthesized Ag/AgCl-NPs showed sufficient efficacy against all tested bacteria. However, their performance did not reach the level achieved by standard antibiotic (Table 1 & Fig. S1). Due to the absence of a protective thick peptidoglycan layer, the outer membrane of gram-negative bacteria is thinner than that of gram-positive bacteria. This allows AgNPs or other drugs to be more destructive towards gram-negative bacteria than to gram-positive bacteria [53]. However, *Staphylococcus aureus* a gram-positive

Table 1
Zone of bacterial growth inhibition by *Maranta arundinacea* rhizome extract-mediated Ag/AgCl-NPs.

Name of the bacteria	Zone of bacterial growth inhibition (mm)						
	Ag/AgCl-NPs (μg/disc)			$AgNO_3$ (μg/disc)			Erythromycin
	10	20	40	10	20	40	15 units
Shigella boydii	8.50 ± 0.57^{o}	9.25 ± 0.95^{o}	$15.50 \pm 0.57^{e\text{-}j}$	$11.00 \pm 0.95^{m\text{-}o}$	$12.25 \pm 0.95^{l\text{-}n}$	$17.75 \pm 0.95^{a\text{-}f}$	20.25 ± 0.50^{a}
Escherichia coli	10.75 ± 0.50^{no}	$13.50 \pm 0.50^{i\text{-}m}$	$17.25 \pm 0.95^{b\text{-}g}$	$13.00 \pm 0.95^{j\text{-}n}$	$15.75 \pm 0.57^{d\text{-}i}$	19.50 ± 0.50^{ab}	19.75 ± 0.57^{ab}
Shigella dysenteriae	$12.25 \pm 0.50^{l\text{-}n}$	$14.50 \pm 0.57^{h\text{-}l}$	$16.50 \pm 1.41^{c\text{-}h}$	$12.50 \pm 0.57^{l\text{-}n}$	$14.75 \pm 0.50^{g\text{-}l}$	$16.75 \pm 0.50^{c\text{-}h}$	$18.75 \pm 0.50^{a\text{-}c}$
Staphylococcus aureus	$14.25 \pm 0.95^{h\text{-}l}$	$15.75 \pm 0.50^{d\text{-}i}$	$18.00 \pm 1.41^{a\text{-}e}$	10.50 ± 0.57^{no}	$12.75 \pm 1.06^{k\text{-}n}$	$15.25 \pm 0.95^{f\text{-}k}$	$18.25 \pm 0.95^{a\text{-}d}$

n = 3 and data are stated as mean ± SD (Standard deviation). Various superscripted letters on the data indicate the significant differences among different concentrations of Ag/AgCl-NPs and erythromycin when $P < 0.05$.

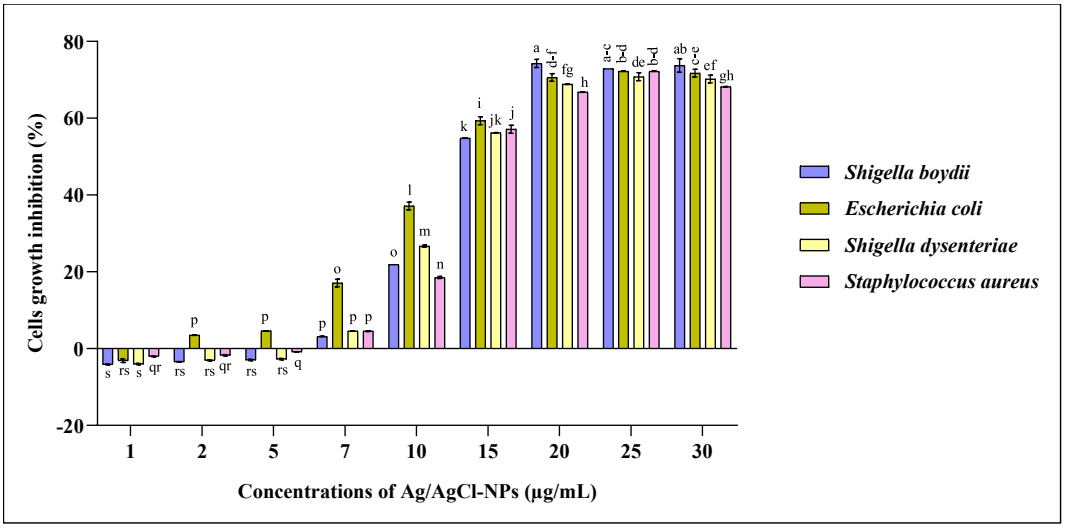

Fig. 4. Minimum inhibitory concentration (MIC) of synthesized Ag/AgCl-NPs for four different bacteria (n = 3 and mean ± SD). Different letters indicate significant differences among various concentrations of Ag/AgCl-NPs when $P < 0.05$.

bacteria showed the highest sensitivity towards the Ag/AgCl-NPs under study. Likewise, leaf extract-mediated Ag/AgCl-NPs of *Mukia maderaspatana* [13] and *Brassica oleracea* [14] showed the highest activity against gram-positive bacteria. This highest antibacterial efficacy against gram-positive bacteria over gram-negative bacteria might be influenced by several factors, such as the size, shape, and concentration of Ag/AgCl-NPs, types of bacterial strains, and experimental conditions [54]. Ag/AgCl-NPs exert antibacterial activity employing a variety of mechanisms such as alteration of the membrane, inhibition of respiration, halting DNA replication, etc. However, the detailed mechanism is still unclear [55]. A study reported that Ag/AgCl-NPs form pits in bacterial cell walls depending on their particle size. After attaching to the bacterial cell wall, a small-sized nanoparticle increases the cell wall permeability, enters into the cell, binds with the functional groups of DNA and proteins, and finally, destroys the cell [56]. At the same time, spherical Ag/AgCl-NPs exhibit more bactericidal efficacy as they can manage better contact with bacterial surface due to having a higher surface area [57]. Another widely acceptable mechanism is the release of Ag^{+} from Ag/AgCl-NPs that are small, and spherical with a large surface area to volume ratio. After an easy penetration into bacterial cells, Ag^{+} interacts with biomolecules, DNA, and proteins that contain thiol groups. As a consequence, cellular activities are impaired, and DNA replication is halted, leading to the loss of cell viability and death in extreme conditions. This mechanism is more widely accepted due to the sustained release of Ag^{+} and Ag^{+} itself possesses a broad-spectrum antimicrobial efficacy [58,59].

3.3.2. MIC of synthesized Ag/AgCl-NPs

The MIC was noted as the lowermost concentration of Ag/AgCl-NPs where no visible growth of bacteria was observed. Fig. 4 shows that the MIC values of synthesized Ag/AgCl-NPs were 2 μg/mL for *Escherichia coli* and 7 μg/mL for *Staphylococcus aureus*, *Shigella dysenteriae,* and *Shigella boydii,* indicating the potential of Ag/AgCl-NPs as antibiotic. Compared to our study, green synthesized Ag/AgCl-NPs from the *Brassica oleracea* showed higher MICs of 25 μg/mL against both *S. aureus* and *E. coli* [14].

3.3.3. Antibiofilm activity of synthesized Ag/AgCl-NPs

The formation of biofilm causes the shifting of acute phase diseases to chronic phase diseases and provides resistance against different antimicrobial agents [12]. *S. aureus*, *E. coli*, *K. pneumoniae*, and *P. aeruginosa* are the most biofilm-forming bacteria associated

Table 2
Antibiofilm activity of *Maranta arundinacea* rhizome extract-mediated Ag/AgCl-NPs against *E. coli*.

Name of the bacteria	Incubation period (h)	Concentrations of Ag/AgCl-NPs (μg/mL)				
		Control	10	20	40	80
Escherichia coli	24	+	+	–	–	–
	48	+	+	–	–	–
	72	+	+	+	–	–
	96	+	+	+	–	–

(+) and (−) indicate the presence and absence of biofilm, respectively.

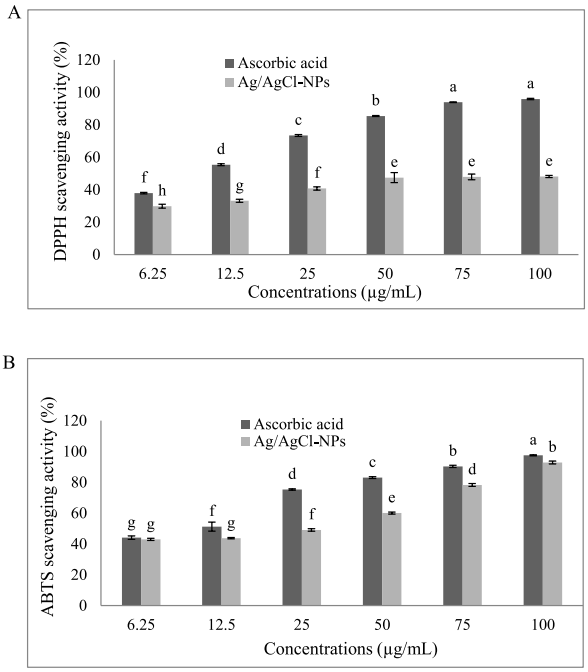

Fig. 5. (A) DPPH and (B) ABTS free radical scavenging activity of synthesized Ag/AgCl-NPs and ascorbic acid as referenced standard (n = 3 and mean ± SD). The significant differences among various concentrations of Ag/AgCl-NPs and ascorbic acid are indicated by different letters on bars when $P < 0.05$.

Table 3
IC_{50} values *Maranta arundinacea* rhizome extract-mediated Ag/AgCl-NPs and standard antioxidant (ascorbic acid) in antioxidant assay.

Types scavenging assay	Ag/AgCl-NPs (μg/mL)	Ascorbic acid (μg/mL)
DPPH scavenging assay	90.65	11.54
ABTS scavenging assay	24.34	10.55

with human infections [60]. In antibiofilm assay, synthesized Ag/AgCl-NPs effectively inhibited the production of biofilm by *E. coli.* The inhibitory effect gradually increased with the concentrations of Ag/AgCl-NPs ranging from 10 to 80 μg/mL. No biofilm was observed for multidrug resistance bacteria *E. coli* during 24–96 h of incubation at 40 μg/mL of Ag/AgCl-NPs (Table 2). A previous research work reported that *Vitis vinifera*-assisted AgNPs showed potent antibiofilm activity against *K. pneumonia* [12]. Another research work has recently reported that *Hypnea musciformis* extract-mediated Ag/AgCl-NPs exhibited antibiofilm activities against *S. mutants* and *S. aureus* [61]. Ag/AgCl-NPs cause permanent damage to bacterial cells, changes in membrane permeability, and respiration during the inhibition of biofilm formation [55].

3.4. Antioxidant activity of synthesized Ag/AgCl-NPs

The antioxidant activity of synthesized Ag/AgCl-NPs was determined using both DPPH and ABTS free radical scavenging assay. The scavenging activities of different concentrations of Ag/AgCl-NPs along with ascorbic acid as standard on DPPH and ABTS free radicals

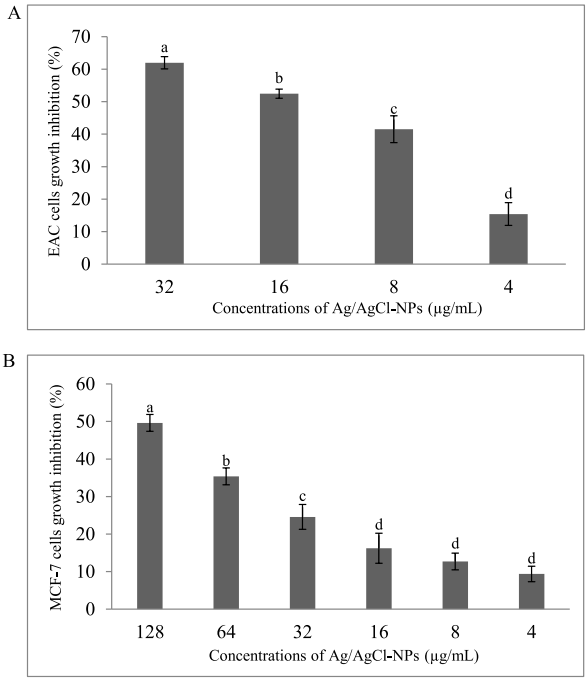

Fig. 6. *In vitro* (A) EAC and (B) MCF-7 cells growth inhibitions (%) by different concentrations of synthesized Ag/AgCl-NPs (n = 3 and mean ± SD). Different letters indicate significant differences among various concentrations of Ag/AgCl-NPs when $P < 0.05$.

are shown in Fig. 5A and B, respectively. At 100 µg/mL concentration of Ag/AgCl-NPs, the recorded scavenging activities were 48.14 % and 92.83 % for DPPH and ABTS, respectively. The scavenging activities were concentration-dependent. The synthesized Ag/AgCl-NPs showed promising antioxidant activity, but it was lower compared to the standard antioxidant (ascorbic acid). This was evidenced by higher IC_{50} values of Ag/AgCl-NPs (DPPH = 90.65 µg/mL and ABTS = 24.34 µg/mL) than that of ascorbic acid (DPPH = 11.54 µg/mL and ABTS = 10.55 µg/mL) (Table 3). A couple of studies stated the similar antioxidant activity of plant extract-based Ag/AgCl-NPs [14,15]. Free radicals cause cellular damage and pause cellular growth by adversely affecting cellular oxidation, a very crucial process. In excess amounts, they direct subversive effects on enzymes like superoxide dismutase, catalase, and peroxidase that protect antioxidants. As a result, cell death occurs due to oxidation of vital biomolecules and finally, via apoptosis. Apart from this, different types of free radicals like oxygen radicals and organic hydroperoxides play a significant role in carcinogenesis. Many tumor promoters cause a cancerous state by inducing a 'pro-oxidant state' in their target tissue [14,15]. Most antioxidants prevent the progression of chronic diseases by repairing the cellular damage caused by free radicals and reactive oxidant species [14]. During the scavenging of free radicals, Ag/AgCl-NPs reduce and neutralize free radicals by donating electrons. Additionally, the high surface area to volume ratio of Ag/AgCl-NPs facilitates the adsorption and neutralization of free radicals [62].

3.5. *In vitro anticancer activity of synthesized Ag/AgCl-NPs against EAC and MCF-7 cells*

Cancer is a group of diseases identified according to their preliminary affected cell types [39]. Recently, several studies reported the anticancer potential of synthesized Ag/AgCl-NPs from plant extract against EAC and MCF-7 cells [10,23,46,61]. In this current experiment, 52.45 % growth of EAC cells was inhibited by 16 µg/mL of Ag/AgCl-NPs. When the concentration was increased to 32 µg/mL, the growth inhibition of EAC cells was also increased to approximately 61.96 % (Fig. 6A). Meanwhile, the growth inhibition of MCF-7 cells was about 35.37 % at 64 µg/mL of Ag/AgCl-NPs. When the concentration was made twice, approximately 49.63 % growth inhibition of MCF-7 cells was observed (Fig. 6B). This result indicated that EAC cells are more sensitive to the Ag/AgCl-NPs than MCF-7 cells. A research work obtained about 87.38 % EAC and 86.75 % MCF-7 cells growth inhibition at 64 µg/mL of green synthesized AgNPs from *Sargassum binderi* [23].

3.6. *In vivo anticancer potential of synthesized Ag/AgCl-NPs against EAC cells*

3.6.1. *In vivo EAC cells growth inhibition by synthesized Ag/AgCl-NPs*

EAC cells resemble human tumors as those are originally hyperdiploid and show high transplantable capability, rapid proliferation, short lifespan, and 100 % malignancy [46]. That's why EAC cells were selected to perform *in vivo* anticancer study. After five consecutive days of treatment with 2.5 and 5 mg/kg/day of synthesized Ag/AgCl-NPs, about 38.30 % and 57.38 % of EAC cells growth inhibition were observed in mice, respectively (Fig. 7A). According to a previous study, at a dose of 12 mg/kg/day,

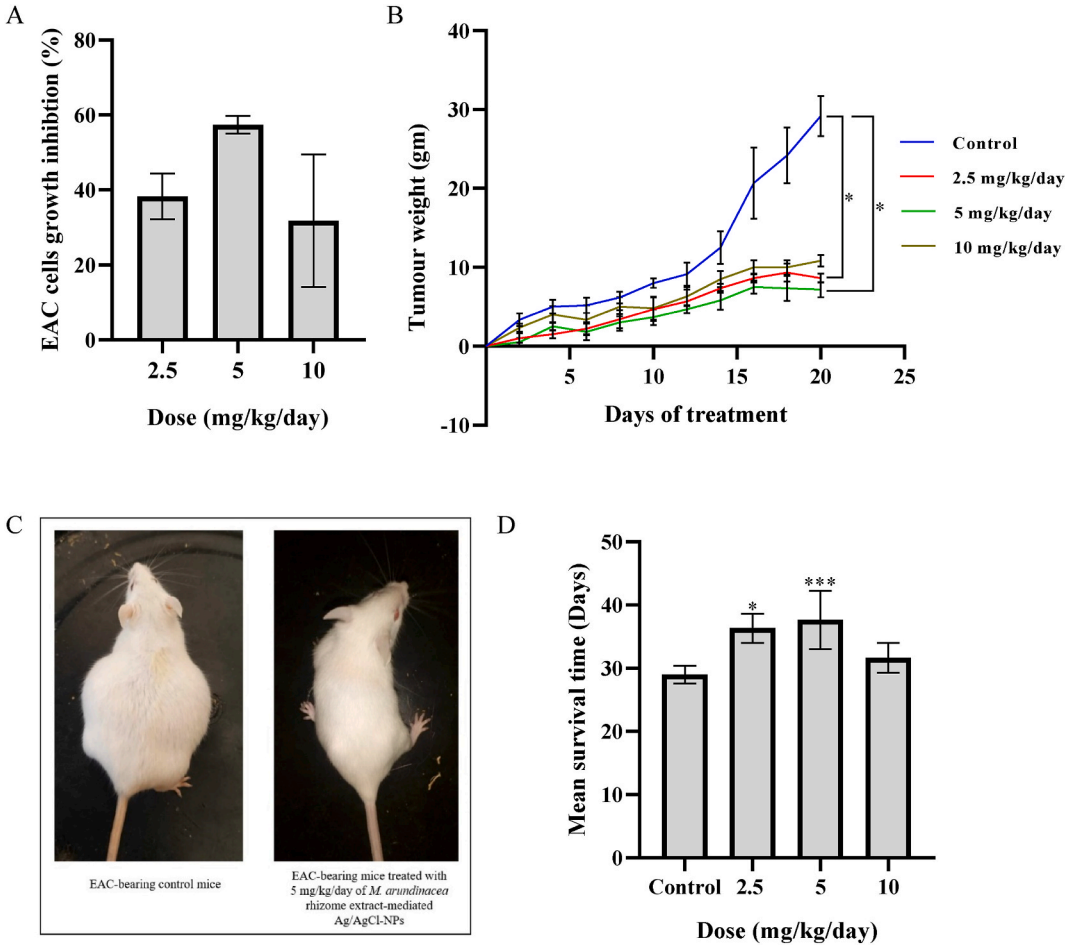

Fig. 7. (A) *In vivo* EAC cells growth inhibition (%) in mice by different doses of synthesized Ag/AgCl-NPs, (B) Average tumor weight (gm), (C) EAC-bearing control and 5 mg/kg/day of Ag/AgCl-NPs treated mice on 20th day of EAC inoculation, and (D) Mean survival time (days) of mice (n = 6 and mean ± SD). *$P < 0.05$ and ***$P < 0.001$, when compared with control.

Z. mauritiana-mediated Ag/AgCl-NPs and *K. rotunda*-mediated Ag/AgCl-NPs inhibited about 20 % and 55 % of EAC cells growth, respectively. But at the dose of 6 mg/kg/day, 0 % and 32.3 % of EAC cells growth inhibitions were exhibited by *Z. mauritiana*-mediated Ag/AgCl-NPs and *K. rotunda*-mediated Ag/AgCl-NPs, respectively [26]. This result indicated the stronger anticancer activity of the Ag/AgCl-NPs under study than *Z. mauritiana*-mediated Ag/AgCl-NPs and *K. rotunda*-mediated Ag/AgCl-NPs. The cytotoxic effect is inversely proportional to the size of Ag/AgCl-NPs. Small Ag/AgCl-NPs can be rapidly accumulated within cells [63]. Probably this is the reason behind the potent cytotoxicity of our small-sized synthesized Ag/AgCl-NPs against EAC cells.

Synthesized Ag/AgCl-NPs showed less potency against cancer at high dose, as evidenced by a surprising decrease in EAC cells growth inhibition to 31.81 % at a high dose of 10 mg/kg/day (Fig. 7A). At high dose Ag/AgCl-NPs exhibited potent toxicity against normal body cells by promoting ROS production, oxidative stress, DNA damage, chromosomal aberration, and finally, cell death via apoptosis [64]. So, at high dose, synthesized Ag/AgCl-NPs probably exert a more lethal effect on normal cells rather than EAC cells. This might explain the obtained decrease in EAC cells growth inhibition when synthesized Ag/AgCl-NPs were administrated at higher dose.

3.6.2. Effect of synthesized Ag/AgCl-NPs on average tumor weight and mean survival time in EAC-bearing mice

Rapidly increased ascites fluid meets the nutritional requirement of EAC cells in EAC-bearing mice [10]. After 10 consecutive days of treatment with 2.5 and 5 mg/kg/day of synthesized Ag/AgCl-NPs, on the 20th day of EAC cells inoculation, the average tumor weight of mice was found to be significantly reduced compared to the control mice due to the decreased volume of ascites fluid and the number of EAC cells (Fig. 7B and C). However, the mean survival time of mice was calculated as higher in the treated groups than in the control group. The treated mice at the doses of 2.5 and 5 mg/kg/day survived approximately 36.33 ± 2.31 and 37.67 ± 4.59 days on average whereas the mice of the control group survived only 29 ± 1.29 days (Fig. 7D). The life span of treated mice at the dose of 5 mg/kg/day increased approximately 30 %. A couple of studies observed similar results [10,24]. But at a high dose of 10 mg/kg/day, Ag/AgCl-NPs showed very poor results in average tumor weight and mean survival time (31.67 ± 2.34 days) possibly due to the

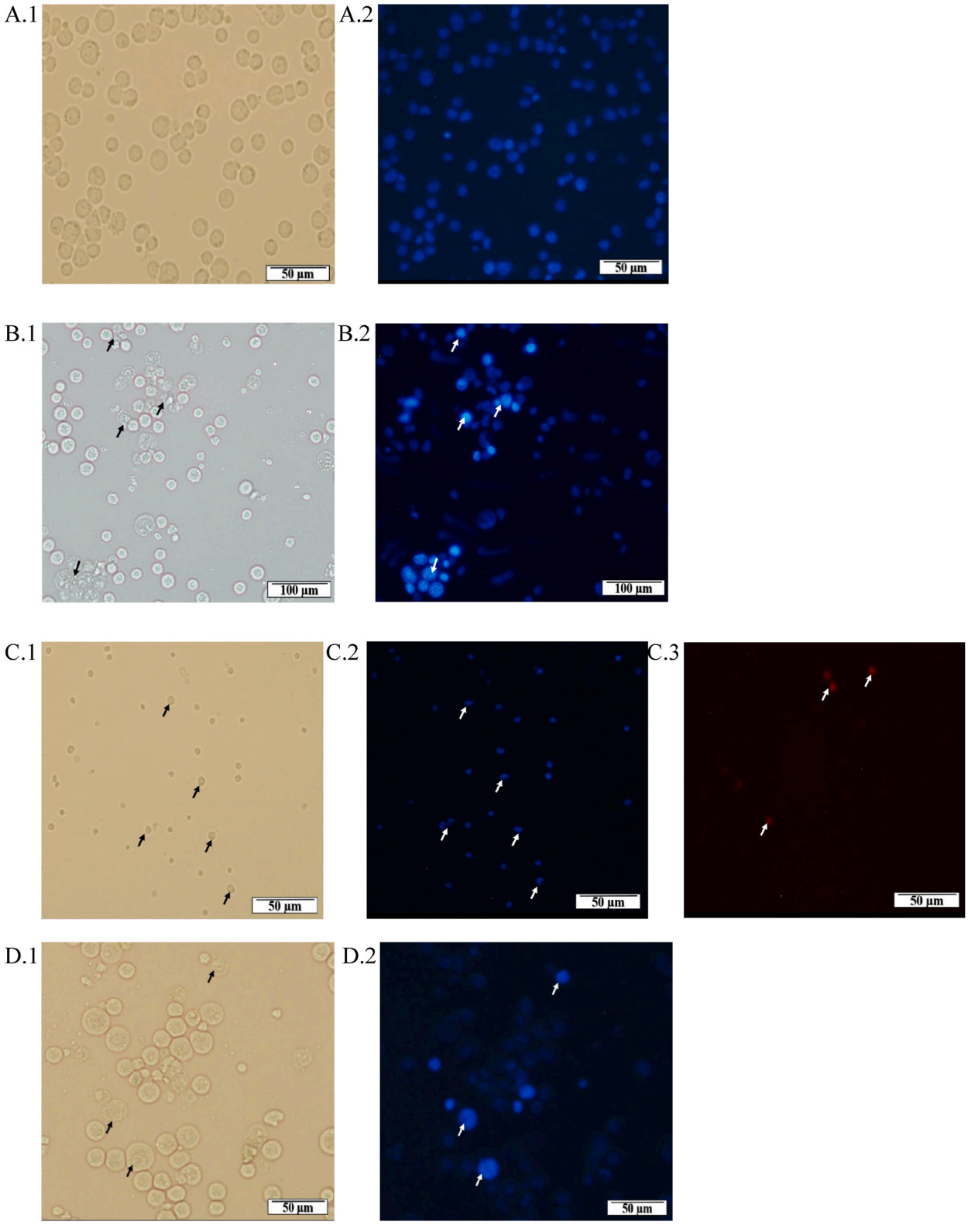

(caption on next page)

Fig. 8. Optical microscopic views of (A.1) Control, (B.1) 2.5 mg/kg/day, (C.1) 5 mg/kg/day, and (D.1) 10 mg/kg/day of synthesized Ag/AgCl-NPs treated EAC cells. Fluorometric views (Hoechst-33342) of (A.2) Control, (B.2) 2.5 mg/kg/day, (C.2) 5 mg/kg/day, and (D.2) 10 mg/kg/day of synthesized Ag/AgCl-NPs treated EAC cells. (C.3) Fluorometric view (Propidium iodide) of EAC cells treated with 5 mg/kg/day of Ag/AgCl-NPs (Arrows indicate apoptotic cells).

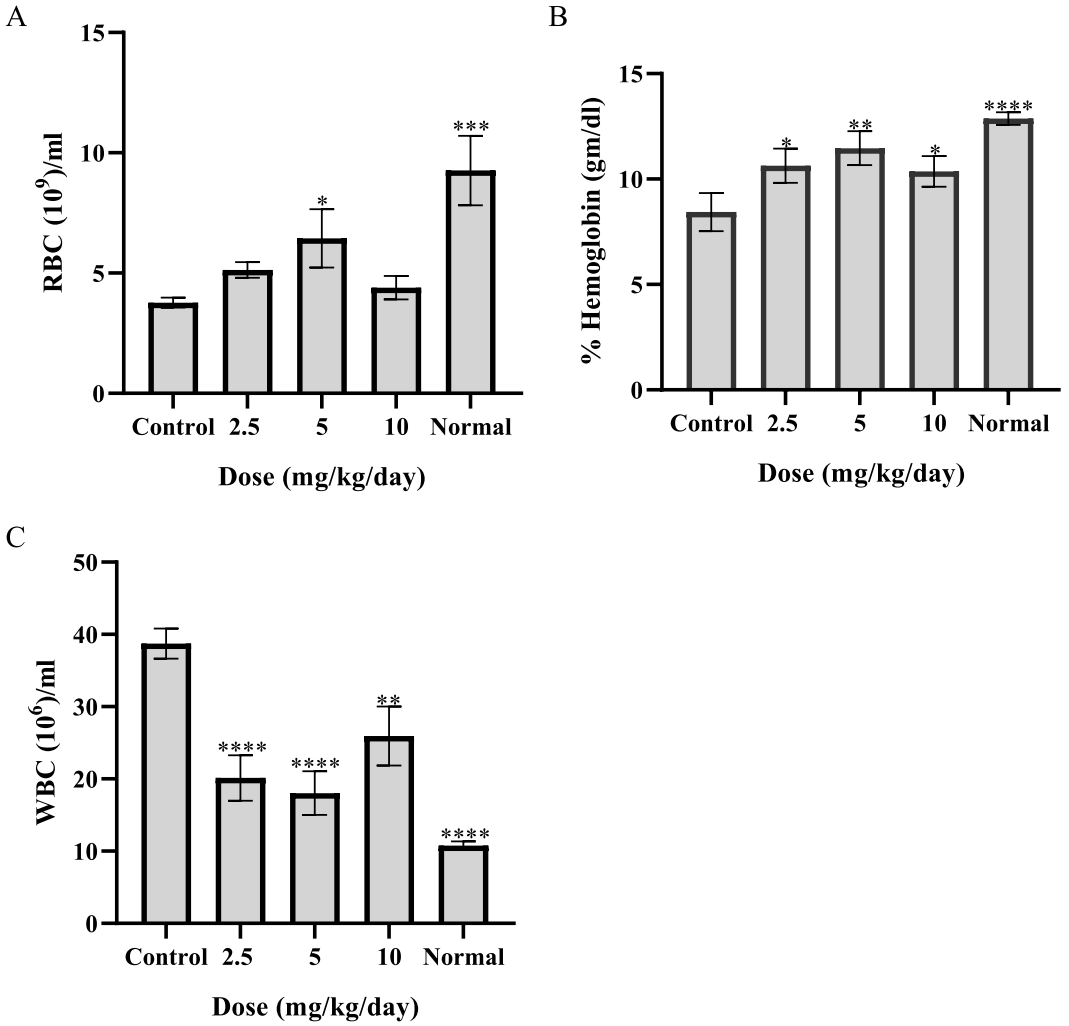

Fig. 9. Changes in (A) Total RBC, (B) % hemoglobin, and (C) Total WBC of mice by different doses of synthesized Ag/AgCl-NPs compared to control (n = 6 and mean ± SD). *$P < 0.05$, **$P < 0.01$, ***$P < 0.001$, and ****$P < 0.0001$, when compared with control.

toxicity in normal body cells rather than in EAC cells. These findings suggest that the synthesized Ag/AgCl-NPs could serve as magnificent candidates for anticancer agents, particularly when administrated at lower doses.

3.6.3. Effect of synthesized Ag/AgCl-NPs on morphological alteration of EAC cells

Both optical and fluorometric images were considered to compare the morphological alterations of EAC cells treated and untreated with synthesized Ag/AgCl-NPs. The size and shape of Ag/AgCl-NPs untreated EAC cells (Fig. 8A.1) were found to be larger and round, respectively. No apoptotic cells were noticed in the fluorometric view (Fig. 8A.2) of untreated EAC cells. On the other hand, Ag/AgCl-NPs treated EAC cells at the doses of 2.5 mg/kg/day (Fig. 8B.1) and 10 mg/kg/day (Fig. 8D.1) were slightly smaller in size and irregular in shape. Additionally, fluorometric views of treated EAC cells at the doses of 2.5 mg/kg/day (Fig. 8B.2) and 10 mg/kg/day (Fig. 8D.2) affirmed the presence of a limited number of apoptotic cells emitting bright blue color. 5 mg/kg/day of Ag/AgCl-NPs was found to be the optimal dose confirmed by the presence of notably small and irregular EAC cells in the optical view (Fig. 8C.1) along with the predominant number of apoptotic cells in the fluorometric views (Fig. 8C.2&C.3). A couple of studies reported the crucial role of plant extract-mediated Ag/AgCl-NPs in eliminating cancer cells by morphological alterations and the induction of apoptosis [23, 65].

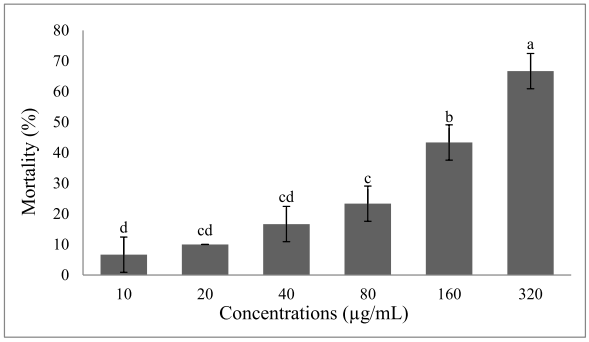

Fig. 10. Cytotoxic activity of synthesized Ag/AgCl-NPs against brine shrimp nauplii (n = 3 and mean ± SD). The significant differences among various concentrations of Ag/AgCl-NPs are indicated by different letters on bars when $P < 0.05$.

3.6.4. Effect of synthesized Ag/AgCl-NPs on hematological parameters in EAC-bearing mice

Typically, anemia occurs in EAC-bearing mice [63]. Our experiment supported this statement because total RBC and hemoglobin levels decreased and total WBC increased in EAC-bearing mice. After 10 days of treatment with synthesized Ag/AgCl-NPs at doses of 2.5 and 5 mg/kg/day, the total RBC (Fig. 9A) and hemoglobin (Fig. 9B) of mice were increased and the total WBC (Fig. 9C) was remarkably decreased compared to control mice. Additionally, all these values of hematological parameters of Ag/AgCl-NPs treated mice were restored close to the values of normal mice. Some studies reported a similar effect of Ag/AgCl-NPs on hematological parameters [63,66]. However, the result was not so impressive at an increased dose of 10 mg/kg/day. A previous study can reveal a possible explanation [64]. Based on this previous study, at high dose, Ag/AgCl-NPs can bind with the RBC surface, cause death, and disturb the maturation of hemoglobin by entering through the membrane.

After injecting Ag/AgCl-NPs into the body, the immune system identifies them as overseas particles and displays a quick reaction, increasing the WBC level. Ag/AgCl-NPs at lower doses are not regarded as severely toxic and the body easily overcame the immunogenic response within a short time, but at a higher dose level, Ag/AgCl-NPs possibly induced severe immunogenic responses which were not compensated and gave rise to a remarkable increase of the WBC level [64].

3.7. Cytotoxicity of synthesized Ag/AgCl-NPs

The synthesized Ag/AgCl-NPs showed moderate toxicity against brine shrimp nauplii with an LC_{50} value of 208.41 µg/mL in the cytotoxicity assay (Fig. 10). This finding indicates that our synthesized Ag/AgCl-NPs are not so toxic to normal body cells. Compared to our synthesized Ag/AgCl-NPs, a study synthesized potent cytotoxic Ag/AgCl-NPs from *Bergenia ciliate* with an LC_{50} value of 33.92 µg/mL [67]. Another study synthesized less cytotoxic Ag/AgCl-NPs from *Lantana camara* L. leaves with an LC_{50} value of 514 µg/mL [68].

4. Conclusion

In the current study, Ag/AgCl-NPs were successfully synthesized from *Maranta arundinacea* rhizome extract which exhibited good antibacterial, antibiofilm, and antioxidant activities with excellent anticancer potential against EAC and MCF-7 cells. Ag/AgCl-NPs also showed tremendously improved hematological parameters in EAC-bearing mice and moderate toxicity against brine shrimp nauplii. Therefore, *M. arundinacea* rhizome extract-mediated Ag/AgCl-NPs have the potential to be used as an antibacterial, antioxidant, and promising anticancer agent in the biomedical sector in the future.

CRediT authorship contribution statement

Md. Ruhul-Amin: Writing – original draft, Methodology, Data curation. **Md. Abdur Rahman:** Methodology. **Nisa Khatun:** Methodology. **Imtiaj Hasan:** Validation. **Syed Rashel Kabir:** Validation, Methodology. **A.K.M. Asaduzzaman:** Writing – review & editing, Supervision, Funding acquisition, Data curation, Conceptualization.

Data availability

Data associated with this study has not been deposited into a publicly available repository but will be made available on request.

Funding

Funding for this research project was provided by the Faculty of Science, University of Rajshahi, Bangladesh. Project No. A-164/5/52/RU/Science-34/2022-2023.

Declaration of competing interest

The authors declare that they have no known competing financial interests.

Acknowledgment

The authors make their positive reception to the Department of Biochemistry and Molecular Biology, Faculty of Science, University of Rajshahi, Bangladesh for funding this research project.

Appendix A. Supplementary data

Supplementary data to this article can be found online at https://doi.org/10.1016/j.heliyon.2024.e39493.

References

[1] S. Ahmed, M. Ahmad, B.L. Swami, S. Ikram, A review on plants extract mediated synthesis of silver nanoparticles for antimicrobial applications: a green expertise, J. Adv. Res. 7 (2016) 17–28, https://doi.org/10.1016/j.jare.2015.02.007.
[2] A.M. Ealias, M.P. Saravanakumar, A review on the classification, characterisation, synthesis of nanoparticles and their application, IOP Conf. Ser. Mater. Sci. Eng. 263 (2017) 1–15, https://doi.org/10.1088/1757-899X/263/3/032019.
[3] I. Khan, K. Saeed, I. Khan, Nanoparticles: properties, applications and toxicities, Arab. J. Chem. 12 (2019) 908–931, https://doi.org/10.1016/j.arabjc.2017.05.011.
[4] T. Giridharan, C. Masi, S. Sindhu, P. Arumugam, Studies on green synthesis, characterization and anti-proliferative potential of silver nano particle using Dodonaea viscosa and Capparis decidua, Biosci. Biotechnol. Res. Asia. 11 (2014) 665–673, https://doi.org/10.13005/bbra/1320.
[5] M.M.H. Khalil, E.H. Ismail, K.Z. El-Baghdady, D. Mohamed, Green synthesis of silver nanoparticles using olive leaf extract and its antibacterial activity, Arab. J. Chem. 7 (2014) 1131–1139, https://doi.org/10.1016/J.ARABJC.2013.04.007.
[6] S. Hasan, A review on nanoparticles : their synthesis and types, Res. J. Recent Sci. 4 (2015) 9–11.
[7] W.I. Abdel-Fattah, G.W. Ali, On the anti-cancer activities of silver nanoparticles, J. Appl. Biotechnol. Bioeng. 5 (2018) 43–46, https://doi.org/10.15406/jabb.2018.05.00116.
[8] X.F. Zhang, Z.G. Liu, W. Shen, S. Gurunathan, Silver nanoparticles: synthesis, characterization, properties, applications, and therapeutic approaches, Int. J. Mol. Sci. 17 (2016) 1–34, https://doi.org/10.3390/ijms17091534.
[9] M.A. Huq, S. Akter, Biosynthesis, characterization and antibacterial application of novel silver nanoparticles against drug resistant pathogenic klebsiella pneumoniae and salmonella enteritidis, Molecules 26 (2021) 1–15, https://doi.org/10.3390/molecules26195996.
[10] S.R. Kabir, F. Islam, A.K.M. Asaduzzaman, Biogenic silver/silver chloride nanoparticles inhibit human cancer cells proliferation in vitro and Ehrlich ascites carcinoma cells growth in vivo, Sci. Rep. 12 (2022) 1–14, https://doi.org/10.1038/s41598-022-12974-z.
[11] T. Bruna, F. Maldonado-Bravo, P. Jara, N. Caro, Silver nanoparticles and their antibacterial applications, Int. J. Mol. Sci. 22 (2021) 1–21, https://doi.org/10.3390/ijms22137202.
[12] A.K.M. Asaduzzaman, B.-S. Chun, S.R. Kabir, Vitis vinifera assisted silver nanoparticles with antibacterial and antiproliferative activity against ehrlich ascites carcinoma cells, J. Nanoparticles. 2016 (2016) 1–9, https://doi.org/10.1155/2016/6898926.
[13] M. Harshiny, M. Matheswaran, G. Arthanareeswaran, S. Kumaran, S. Rajasree, Enhancement of antibacterial properties of silver nanoparticles–ceftriaxone conjugate through Mukia maderaspatana leaf extract mediated synthesis, Ecotoxicol. Environ. Saf. 121 (2015) 135–141, https://doi.org/10.1016/J.ECOENV.2015.04.041.
[14] S. Ansar, H. Tabassum, N.S.M. Aladwan, M. Naiman Ali, B. Almaarik, S. AlMahrouqi, M. Abudawood, N. Banu, R. Alsubki, Eco friendly silver nanoparticles synthesis by Brassica oleracea and its antibacterial, anticancer and antioxidant properties, Sci. Rep. 10 (2020) 1–12, https://doi.org/10.1038/s41598-020-74371-8.
[15] S. Kota, P. Dumpala, R.K. Anantha, M.K. Verma, S. Kandepu, Evaluation of therapeutic potential of the silver/silver chloride nanoparticles synthesized with the aqueous leaf extract of Rumex acetosa, Sci. Rep. 7 (2017) 1–11, https://doi.org/10.1038/s41598-017-11853-2.
[16] R.M. Isleem, M.M. Alzaharna, F.A. Sharif, Synergistic anticancer effect of combining metformin with olive (Olea europaea L.) leaf crude extract on the human breast cancer cell line MCF-7 Rajy M Isleem, Mazen M Alzaharna and Fadel A Sharif, J. Med. Plants Stud. 8 (2020) 30–37. www.plantsjournal.com.
[17] Y. Cai, B. Karmakar, M.A. Salem, A.Y. Alzahrani, M.Z. Bani-Fwaz, A.A.A. Oyouni, O. Al-Amer, G.E.S. Batiha, Ag NPs supported chitosan-agarose modified Fe3O4 nanocomposite catalyzed synthesis of indazolo[2,1-b]phthalazines and anticancer studies against liver and lung cancer cells, Int. J. Biol. Macromol. 208 (2022) 20–28, https://doi.org/10.1016/j.ijbiomac.2022.02.172.
[18] J.-W. Choi, T.N.M. Hua, Impact of lifestyle behaviors on cancer risk and prevention, J. Lifestyle Med. 11 (2021) 1–7, https://doi.org/10.15280/jlm.2021.11.1.1.
[19] H.I.O. Gomes, C.S.M. Martins, J.A. V Prior, Silver nanoparticles as carriers of anticancer drugs for efficient target treatment of cancer cells, Nanomaterials 11 (2021) 1–31, https://doi.org/10.3390/nano11040964.
[20] K. Jeyaprakash, M.S. Alsalhi, S. Devanesan, Anticancer and antioxidant efficacy of silver nanoparticles synthesized from fruit of Morinda citrifolia Linn on Ehrlich ascites carcinoma mice, J. King Saud Univ. Sci. 32 (2020) 3181–3186, https://doi.org/10.1016/j.jksus.2020.09.005.
[21] D.T. Debela, S.G.Y. Muzazu, K.D. Heraro, M.T. Ndalama, B.W. Mesele, D.C. Haile, S.K. Kitui, T. Manyazewal, New approaches and procedures for cancer treatment: current perspectives, SAGE Open Med 9 (2021) 1–10, https://doi.org/10.1177/20503121211034366.
[22] J.S. Devi, V. Bhimba, K. Ratnam, In vitro anticancer activity of silver nanoparticles synthesized using the extract of Gelidiella sp, Int. J. Pharm. Pharm. Sci. 4 (2012) 710–715.
[23] M.S. Ahamed, M.M. Rahman, I. Hasan, S.R. Kabir, A.K.M. Asaduzzaman, Antiproliferative potential of Sargassum binderi Sonder ex J. Agardh mediated biogenic silver/silver chloride nanoparticles on EAC, MCF-7 and HCT116 cells, Indian J. Geo Mar. Sci. 51 (2022) 126–137.
[24] S.R. Kabir, F. Islam, A.A. Al-bari, A.K.M. Asaduzzaman, Asparagus racemosus mediated silver chloride nanoparticles induce apoptosis in glioblastoma stem cells in vitro and inhibit Ehrlich ascites carcinoma cells growth in vivo, Arab. J. Chem. 15 (2022) 1–13, https://doi.org/10.1016/j.arabjc.2022.104013.
[25] M. Oves, M. Aslam, M.A. Rauf, S. Qayyum, H.A. Qari, M.S. Khan, M.Z. Alam, S. Tabrez, A. Pugazhendhi, I.M.I. Ismail, Antimicrobial and anticancer activities of silver nanoparticles synthesized from the root hair extract of Phoenix dactylifera, Mater. Sci. Eng. C. 89 (2018) 429–443, https://doi.org/10.1016/j.msec.2018.03.035.
[26] S.R. Kabir, Z. Dai, M. Nurujjaman, X. Cui, A.K.M. Asaduzzaman, B. Sun, X. Zhang, H. Dai, X. Zhao, Biogenic silver/silver chloride nanoparticles inhibit human glioblastoma stem cells growth in vitro and Ehrlich ascites carcinoma cell growth in vivo, J. Cell Mol. Med. 24 (2020) 13223–13234, https://doi.org/10.1111/jcmm.15934.
[27] N. Sultana, M. Ruhul-Amin, I. Hasan, S.R. Kabir, A.K.M. Asaduzzaman, Antibacterial , antioxidant , and anticancer effects of green synthesized silver/silver chloride nanoparticles using Spondias pinnata bark extract, Food Chem. Adv 4 (2024) 100709, https://doi.org/10.1016/j.focha.2024.100709.

[28] N. Firoskhan, R. Muthuswamy, Review on maranta arundinacea L . (marantacea) international journal of pharmacognosy and pharmaceutical research, Int. J. Pharmacogn. Pharm. Res. 3 (2021) 1–4.

[29] J. Tarique, S.M. Sapuan, A. Khalina, S.F.K. Sherwani, J. Yusuf, R.A. Ilyas, Recent developments in sustainable arrowroot (Maranta arundinacea Linn) starch biopolymers , fibres , biopolymer composites and their potential industrial applications : a review, J. Mater. Res. Technol. 13 (2021) 1191–1219, https://doi.org/10.1016/j.jmrt.2021.05.047.

[30] S. Pv, R. Vv, M. Kv, Pharmacognostic standardisation of Maranta arundinacea L . - an important ethnomedicine, J. Pharmacogn. Phytochem. 4 (2015) 242–246.

[31] A. Jayakumar, A. Suganthi, Biochemical and phytochemical analysis of maranta arundinacea (L .) Rhizome, Int. J. Res. Pharm. Pharm. Sci. 2 (2017) 26–30.

[32] R. Algotiml, A. Gab-Alla, R. Seoudi, H.H. Abulreesh, M.Z. El-Readi, K. Elbanna, Anticancer and antimicrobial activity of biosynthesized Red Sea marine algal silver nanoparticles, Sci. Rep. 12 (2022) 1–18, https://doi.org/10.1038/s41598-022-06412-3.

[33] M.G. Syahputra, A.L. Antari, E.S. Lestari, Antimicrobial effect of arrowroot (Maranta arundinacea L.) methanolic extract against Staphylococcus aureus bacterial growth, Diponegoro Med. J. 9 (2020) 241–245.

[34] N. Khatun, M. Ruhul-Amin, S. Parvin, A. Siddika, I. Hasan, S.R. Kabir, A.K.M. Asaduzzaman, Green synthesis of silver/silver chloride nanoparticles derived from Elaeocarpus floribundus leaf extract and study of its anticancer potential against EAC and MCF-7 cells with antioxidant and antibacterial properties, Results, Chem 7 (2024) 101287, https://doi.org/10.1016/j.rechem.2023.101287.

[35] S.R. Kabir, A.K.M. Asaduzzaman, R. Amin, A.T. Haque, R. Ghose, M.M. Rahman, J. Islam, M.B. Amin, I. Hasan, T. Debnath, B.S. Chun, X.D. Zhao, M.K. Rahman Khan, M.T. Alam, Zizyphus mauritiana fruit extract-mediated synthesized silver/silver chloride nanoparticles retain antimicrobial activity and induce apoptosis in MCF-7 cells through the fas pathway, ACS Omega 5 (2020) 20599–20608, https://doi.org/10.1021/acsomega.0c02878.

[36] S.S. Pallavi, H.A. Rudayni, A. Bepari, S.K. Niazi, S. Nayaka, Green synthesis of Silver nanoparticles using Streptomyces hirsutus strain SNPGA-8 and their characterization, antimicrobial activity, and anticancer activity against human lung carcinoma cell line A549, Saudi J. Biol. Sci. 29 (2022) 228–238, https://doi.org/10.1016/j.sjbs.2021.08.084.

[37] M. Khatun, Z. Khatun, M.R. Karim, M.R. Habib, M.H. Rahman, M.A. Aziz, Green synthesis of silver nanoparticles using extracts of Mikania cordata leaves and evaluation of their antioxidant, antimicrobial and cytotoxic properties, Food Chem. Adv 3 (2023) 100386, https://doi.org/10.1016/j.focha.2023.100386.

[38] I. Hasan, Y. Ozeki, S.R. Kabir, Purification of a novel chitin-binding lectin with antimicrobial and antibiofilm activities from a Bangladeshi cultivar of potato (Solanum tuberosum), Indian J. Biochem. Biophys. 51 (2014) 142–148.

[39] N. Arfin, M.K. Podder, S.R. Kabir, A.K.M. Asaduzzaman, I. Hasan, Antibacterial , antifungal and in vivo anticancer activities of chitin-binding lectins from Tomato (Solanum lycopersicum) fruits, Arab. J. Chem. 15 (2022) 1–10, https://doi.org/10.1016/j.arabjc.2022.104001.

[40] N. Mukaratirwa-muchanyereyi, C. Gusha, M. Mujuru, U. Guyo, S. Nyoni, Synthesis of silver nanoparticles using plant extracts from Erythrina abyssinica aerial parts and assessment of their anti-bacterial and anti-oxidant activities, Results, Chem 4 (2022) 100402, https://doi.org/10.1016/j.rechem.2022.100402.

[41] D. Zheleva-Dimitrova, P. Nedialkov, G. Kitanov, Radical scavenging and antioxidant activities of methanolic extracts from Hypericum species growing in Bulgaria, Pharmacogn. Mag. 6 (2010) 74–78, https://doi.org/10.4103/0973-1296.62889.

[42] S.R. Kabir, M.M. Rahman, S. Tasnim, M.R. Karim, N. Khatun, I. Hasan, R. Amin, S.S. Islam, A.K.M. Asaduzzaman, Purification and characterization of a novel chitinase from Trichosanthes dioica seed with antifungal activity, Int. J. Biol. Macromol. 84 (2016) 62–68, https://doi.org/10.1016/j.ijbiomac.2015.12.006.

[43] S. Rana, S. Rahman, S. Sana, T.K. Biswas, A.K.M. Hashem, S. Parvin, K. Mazumder, Anticancer potential of Chenopodium album leaf extract against Ehrlich ascites carcinoma cells in Swiss albino mice, Futur. J. Pharm. Sci. 6 (2020) 1–9, https://doi.org/10.1186/s43094-020-00080-8.

[44] D.J. Finney, Probit Analysis, in: Fourth, Cambridge University Press, London, 1971, p. 333.

[45] K.L. Kelly, E. Coronado, L.L. Zhao, G.C. Schatz, The optical properties of metal nanoparticles: the influence of size, shape, and dielectric environment, J. Phys. Chem. B 107 (2003) 668–677, https://doi.org/10.1021/jp026731y.

[46] B.K. Srinivas, M.C. Shivamadhu, K.K. Siddappaji, D.K. Krishnappa, S. Jayarama, Angiosuppressive effects of bio - fabricated silver nanoparticles synthesis using Clitoria ternatea flower : an in vitro and in vivo approach, J. Biol. Inorg. Chem. 24 (2019) 1115–1126, https://doi.org/10.1007/s00775-019-01721-x.

[47] A. Bankar, B. Joshi, A.R. Kumar, S. Zinjarde, Banana peel extract mediated novel route for the synthesis of silver nanoparticles, Colloids Surfaces A Physicochem. Eng. Asp. 368 (2010) 58–63, https://doi.org/10.1016/J.COLSURFA.2010.07.024.

[48] R. Mariselvam, A.J.A. Ranjitsingh, A. Usha Raja Nanthini, K. Kalirajan, C. Padmalatha, P. Mosae Selvakumar, Green synthesis of silver nanoparticles from the extract of the inflorescence of Cocos nucifera (Family: arecaceae) for enhanced antibacterial activity, Spectrochim. Acta Part A Mol. Biomol. Spectrosc. 129 (2014) 537–541, https://doi.org/10.1016/J.SAA.2014.03.066.

[49] K. Okaiyeto, M.O. Ojemaye, H. Hoppe, L. V Mabinya, A.I. Okoh, Phytofabrication of silver/silver chloride oedera genistifolia : characterization and antibacterial potential, Molecules 24 (2019) 1–15.

[50] S. Raja, V. Ramesh, V. Thivaharan, Green biosynthesis of silver nanoparticles using Calliandra haematocephala leaf extract , their antibacterial activity and hydrogen peroxide sensing capability, Arab. J. Chem. 10 (2015) 253–261, https://doi.org/10.1016/j.arabjc.2015.06.023.

[51] B. Ajitha, Y. Ashok Kumar Reddy, P.S. Reddy, Biogenic nano-scale silver particles by Tephrosia purpurea leaf extract and their inborn antimicrobial activity, Spectrochim. Acta Part A Mol. Biomol. Spectrosc. 121 (2014) 164–172, https://doi.org/10.1016/j.saa.2013.10.077.

[52] W. Yang, C. Yang, M. Sun, F. Yang, Y. Ma, Z. Zhang, X. Yang, Green synthesis of nanowire-like Pt nanostructures and their catalytic properties, Talanta 78 (2009) 557–564, https://doi.org/10.1016/J.TALANTA.2008.12.009.

[53] G. Singh, P.K. Babele, S.K. Shahi, R.P. Sinha, M.B. Tyagi, A. Kumar, Green synthesis of silver nanoparticles using cell extracts of anabaena doliolum and screening of its antibacterial and antitumor activity, J. Microbiol. Biotechnol. 24 (2014) 1366–1379, https://doi.org/10.4014/jmb.1405.05003.

[54] J.R. Morones, J.L. Elechiguerra, A. Camacho, K. Holt, J.B. Kouri, J.T. Ramírez, M.J. Yacaman, The bactericidal effect of silver nanoparticles, Nanotechnology 16 (2005) 2346–2353, https://doi.org/10.1088/0957-4484/16/10/059.

[55] G. Franci, A. Falanga, S. Galdiero, L. Palomba, M. Rai, G. Morelli, M. Galdiero, Silver nanoparticles as potential antibacterial agents, Molecules 20 (2015) 8856–8874, https://doi.org/10.3390/molecules20058856.

[56] V.K. Sharma, R.A. Yngard, Y. Lin, Silver nanoparticles : green synthesis and their antimicrobial activities, Adv. Colloid Interface Sci. 145 (2009) 83–96, https://doi.org/10.1016/j.cis.2008.09.002.

[57] S. Pal, Y.K. Tak, J.M. Song, Does the antibacterial activity of silver nanoparticles depend on the shape of the nanoparticle? A study of the gram-negative bacterium Escherichia coli, Appl. Environ. Microbiol. 73 (2007) 1712–1720, https://doi.org/10.1128/AEM.02218-06.

[58] M. Sharifi-Rad, P. Pohl, F. Epifano, Phytofabrication of silver nanoparticles (Agnps) with pharmaceutical capabilities using otostegia persica (burm.) boiss. leaf extract, Nanomaterials 11 (2021), https://doi.org/10.3390/nano11041045.

[59] N. Durán, M. Durán, M.B. de Jesus, A.B. Seabra, W.J. Fávaro, G. Nakazato, Silver nanoparticles: a new view on mechanistic aspects on antimicrobial activity, Nanomedicine Nanotechnology, Biol. Med. 12 (2016) 789–799, https://doi.org/10.1016/j.nano.2015.11.016.

[60] R.M. Donlan, J.W. Costerton, Biofilms : survival mechanisms of clinically relevant microorganisms, Clin. Microbiol. Rev. 15 (2002) 167–193, https://doi.org/10.1128/CMR.15.2.167.

[61] R. Ghose, A.K.M. Asaduzzaman, I. Hasan, S.R. Kabir, Hypnea musciformis - mediated Ag/AgCl - NPs inhibit pathogenic bacteria, HCT - 116 and MCF - 7 cells' growth in vitro and Ehrlich ascites carcinoma cells in vivo in mice, IET Nanobiotechnol. 16 (2022) 49–60, https://doi.org/10.1049/nbt2.12075.

[62] A.K. Mittal, A. Kaler, U.C. Banerjee, Free radical scavenging and antioxidant activity of silver nanoparticles synthesized from flower extract of Rhododendron dauricum, Nano Biomed. Eng. 4 (2012) 118–124, https://doi.org/10.5101/nbe.v4i3.p118-124.

[63] N.E.-A. El-Naggar, M.H. Hussein, A.A. El-Sawah, Bio-fabrication of silver nanoparticles by phycocyanin , characterization , in vitro anticancer activity against breast cancer cell line and in vivo cytotxicity, Sci. Rep. 7 (2017) 1–20, https://doi.org/10.1038/s41598-017-11121-3.

[64] D.K. Tiwari, T. Jin, J. Behari, Dose-dependent in-vivo toxicity assessment of silver nanoparticle in Wistar rats, Toxicol. Mech. Methods 21 (2011) 13–24, https://doi.org/10.3109/15376516.2010.529184.

[65] B.C.G. Selvi, J. Madhavan, A. Santhanam, Cytotoxic effect of silver nanoparticles synthesized from padina tetrastromatica on breast cancer cell line, Adv. Nat. Sci. Nanosci. Nanotechnol. 7 (2016) 1–8, https://doi.org/10.1088/2043-6262/7/3/035015.

[66] R. Kumari, A.K. Saini, A.K. Chhillar, V. Saini, R.V. Saini, Antitumor effect of bio-fabricated silver nanoparticles towards ehrlich ascites carcinoma, Biointerface Res. Appl. Chem. 11 (2021) 12958–12972, https://doi.org/10.33263/BRIAC115.1295812972.
[67] A.-R. Phull, Q. Abbas, A. Ali, H. Raza, S.J. kim, M. Zia, I. Haq, Antioxidant, cytotoxic and antimicrobial activities of green synthesized silver nanoparticles from crude extract of Bergenia ciliata, Futur. J. Pharm. Sci. 2 (2016) 31–36, https://doi.org/10.1016/j.fjps.2016.03.001.
[68] P.S.P, K.S.T, Antioxidant, antibacterial and cytotoxic potential of silver nanoparticles synthesized using terpenes rich extract of Lantana camara L. leaves, Biochem. Biophys. Reports. 10 (2017) 76–81, https://doi.org/10.1016/J.BBREP.2017.03.002.